Thermal Fatigue Resistance of Discontinuously Reinforced Cast Aluminum-Matrix Composites

J. Sobczak, Z. Slawinski, N. Sobczak, P. Darlak, R. Asthana, and P. Rohatgi

(Submitted 3 January 2002; in revised form 20 May 2002)

The thermal fatigue resistance of AlSi alloys and discontinuously reinforced Al-matrix composites containing graphite, silicon carbide, and fly ash particulates, and short alumina (Saffil) fibers was characterized by measuring the total length of microcracks on gravity-cast and squeeze-cast test specimens as a function of number of thermal cycles (1000-5000 cycles, 270 K amplitude). In each thermal cycle, the test specimens were heated and stabilized in air at 375 °C, water quenched, and air stabilized. In all specimens, the total crack length on a specified region increased with increasing number of thermal cycles. Whereas among monolithic alloys, squeeze-cast Al-12SiCuNiMg alloy exhibited better resistance to thermal cracking than Al-25Si and Al-20SiNi alloys, among the composites, squeeze-cast Al-alumina and Al-fly ash composites exhibited the best thermal fatigue resistance. The theoretical estimates of the thermal fatigue resistance of these composites are consistent with the experimental observations.

Keywords cast composites, fly ash, squeeze casting, thermal expansion, thermal fatigue

1. Introduction

Material degradation due to thermal cycling has been observed in a wide variety of continuous fiber-reinforced metals such as C/Al, W/Cu, W/superalloys, alumina/superalloy, B/Al, alumina (FP)/Al and others.[1-6] In contrast, the thermal cycling data on discontinuous composites reinforced with short fibers, whiskers, and particulates are rather limited.[7-9] Recent interest in discontinuously reinforced cast composites in the automotive industry has focused attention on their physical and mechanical properties, including thermal fatigue resistance. For example, Kolbenschmidt AG, Germany, in cooperation with Dider-Werke AG, has investigated the thermal shock resistance of squeeze cast KS-1275[1] (AlSi12CuMgNi) piston alloy composites reinforced with Al_2O_3 short fibers and SiC whiskers.[10,11] The composites were fabricated by infiltrating the KS 1275 alloy into porous Al_2O_3 and SiC preforms (80 vol.% porosity), followed by solidification under high pressures to form KS 1275/20 vol.% Al_2O_3 and KS 1275/20 vol.% SiC composites. The thermal shock resistance was estimated from the summarized length of all cracks on thermally cycled test specimens (Fig. 1). These investigations showed that short fiber- and whisker-reinforced composites possessed better resistance to crack propagation than the squeezecast monolithic alloy.

The objective of the present work was to investigate the thermal shock resistance of cast AlSi alloys and Al-matrix composites containing graphite, silicon carbide, fly ash particulates, and short alumina (Saffil) fibers following the crack length measurement approach presented in Ref. 10. The composites were fabricated using the squeeze casting approach described in Ref. 11.

2. Experimental Procedure

The thermal fatigue tests were carried out at Foundry Research Institute (Krakow, Poland) using a fully automated prototype thermal cycling setup. The monolithic and composite test specimens were attached to threaded corrosion-resistant steel tubes with type K (CrNi-Ni) thermocouples inside each sample (Fig. 2a). The thermocouples were encased in ceramic tubes (outer diameter, 2.5 mm). The steel tubes carrying the test specimens were mounted on a movable shoulder, capable of holding 20 test specimens and were thermally cycled (Fig. 2b) as follows: heated in a resistance furnace up to a specified temperature, stabilized in air, submerged in running water, and dried in air. The temperature was measured using a PC thermo recorder. The maximal temperature scatter in the samples was ±15 °C. Each reported datum is an average of measurements on three samples of the same material. The thermal shock resistance was characterized as the total (summarized) length of all microcracks on the bottom face of each sample after a specified number of thermal cycles. The crack lengths were measured using a microscopic magnifier (±0.1 mm accuracy). The test materials used in the study are listed in Table 1. All materials were either gravity cast in permanent molds or squeeze cast, followed by T6 heat treatment[2] prior to thermal cycling.

3. Results and Discussion

Figure 2(c) shows the relation between total crack length and number of thermal cycles for all test materials, and Fig. 3-5

J. Sobczak, N. Sobczak, and **P. Darlak,** Foundry Research Institute, 73 Zakopianska St., 30-418 Krakow, Poland; **Z. Slawinski,** Technical University of Lublin, 36 Nadbystrzycka St., 20-618 Lublin, Poland; **R. Asthana,** Manufacturing Engineering, Technology Dept., University of Wisconsin-Stout, Menomonie, WI 54751; and **P. Rohatgi,** Materials Department, University of Wisconsin-Milwaukee, Milwaukee, WI 53201. Contact e-mail: asthanar@uwstout.edu.

[1]In Germany, DIN 1725

[2]T6 heat treatment: solutionize at 515 C for 6 h, cool in hot water, age at 170 C for 16 h, follow by air cooling.

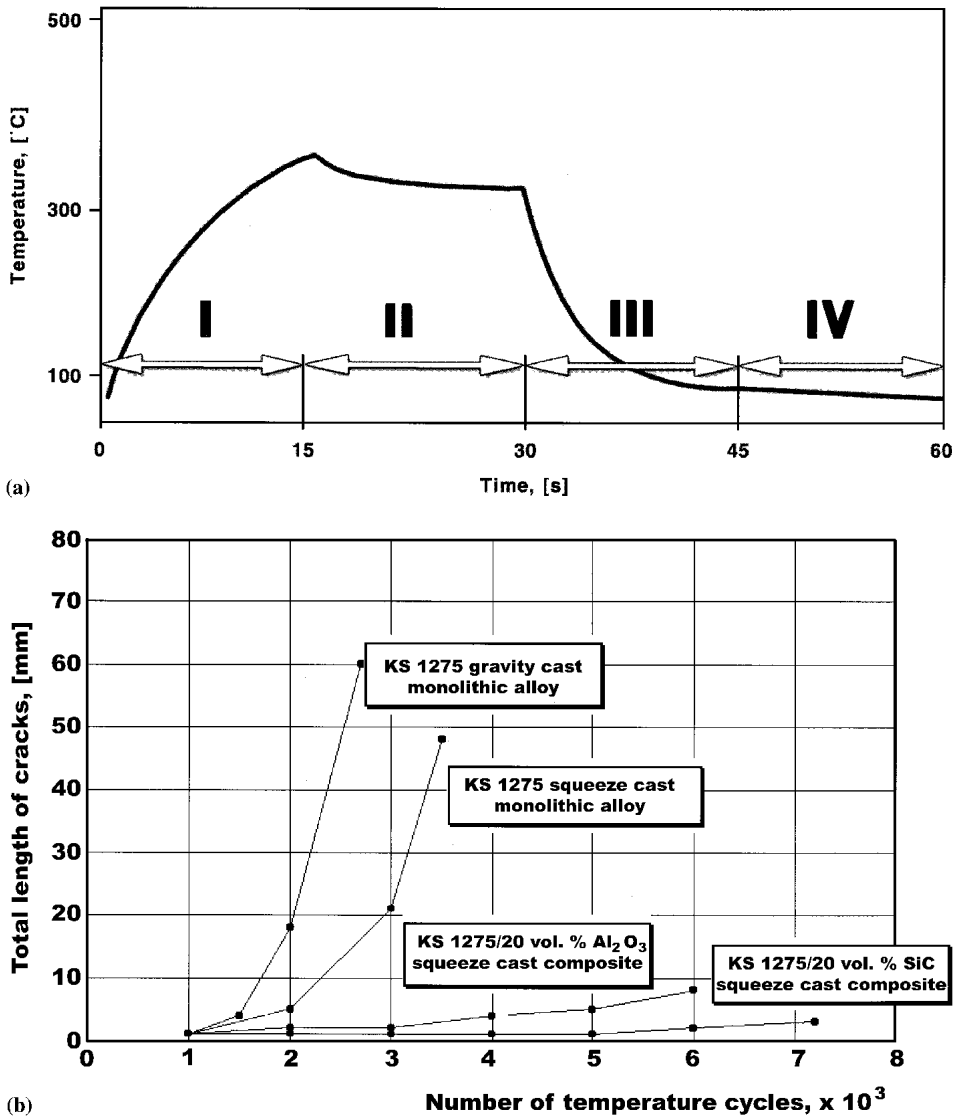

Fig. 1 **(a)** Temperature excursions and **(b)** thermal shock resistance (total crack length) for KS 1275 (AlSi12CuNiMg) piston alloy and its composites reported by Kolbenschmidt AG and Didier-Werke AG, Germany[10]

display photographs of analyzed (bottom) faces of tested specimens. Photomicrographs showing crack propagation in monolithic (AlSi12CuNiMg) alloy, and reinforced (AlSi12CuNiMg/22 vol.% Al_2O_3) squeeze-cast composites are shown in Fig. 6. Figure 2(c) shows that relatively low thermal shock resistance was typical of permanent mold cast monolithic hypereutectic alloys AlSi25 and AlSi20Ni. The higher silicon content (more primary Si) in these alloys led to longer total crack length and inferior thermal shock resistance. Among all tested monolithic materials, squeezecast (T6) AlSi12CuNiMg alloy exhibited the best thermal shock resistance. The application of high external pressures during crystallization and the subsequent T6 heat treatment led to improved structure and chemical homogeneity.[8] Additionally, alloying elements like Cu and Ni in the alloy AlS12CuNiMg are beneficial to the mechanical properties of this typical piston alloy.

The incorporation of 5.7 wt.% graphite in the AlSi20Ni alloy slightly decreased its thermal shock resistance; whereas in the squeeze cast (T6) AlSi12CuNiMg alloy, the effect of the same amount of graphite is far more detrimental. On the other hand, the SiC reinforced-AlSi10Mg (A359) composite exhibited a behavior with respect to change in crack length with number of temperature cycles similar to the AlSi12CuNiMg alloy. The thermal cycling of AlSi12CuNiMg alloy led to visible deformation of tested specimens contrary to the F3S.20S Duralcan composite where no deformation was observed. The best thermal shock resistance (i.e., minimum total crack length) was exhibited by AlSi12CuNiMg/10.36 vol.% fly ash and AlSi12CuNiMg/22 vol.% short Al_2O_3 fiber composites (Fig. 2c). These reinforcements appeared to almost completely stop the propagation of microcracks.

The crack propagation in a two-phase monolithic material can proceed in several different ways (Fig. 7 a): (1) through α-phase and β-phase, (2) along grains boundaries, (3) through gas-shrinkage pores, (4) through α-phase only, and (5) through second-phase precipitates. On the other hand, in metal-matrix composites, these crack propagation mechanisms are supplemented by additional ones due to the presence of the reinforce-

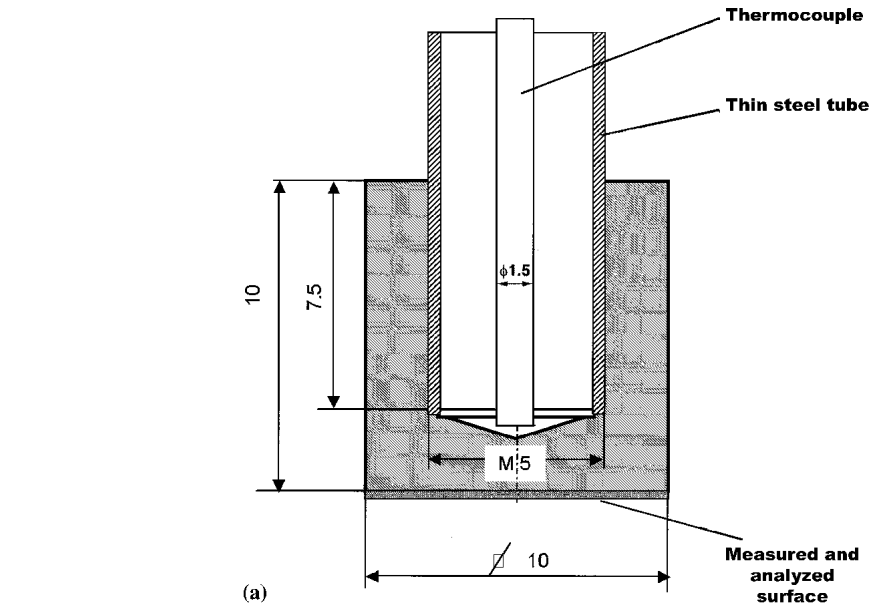

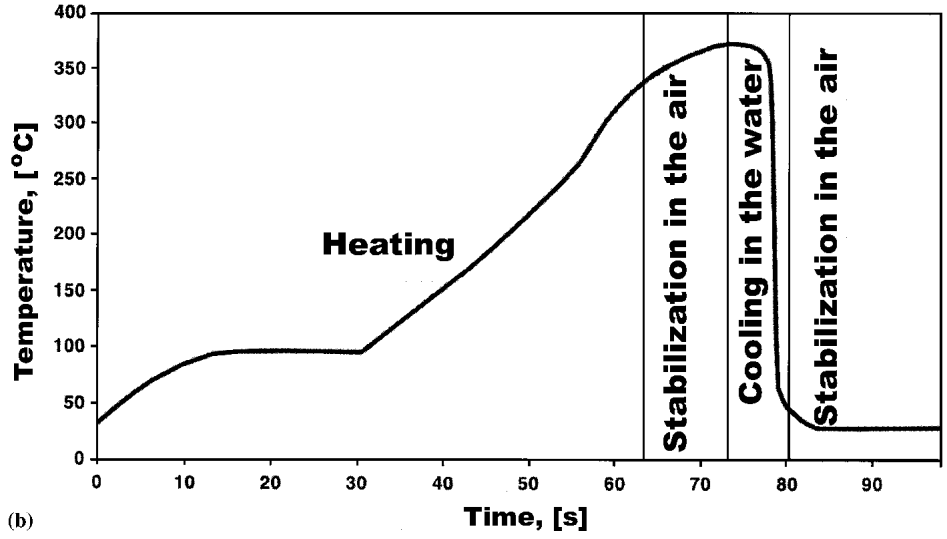

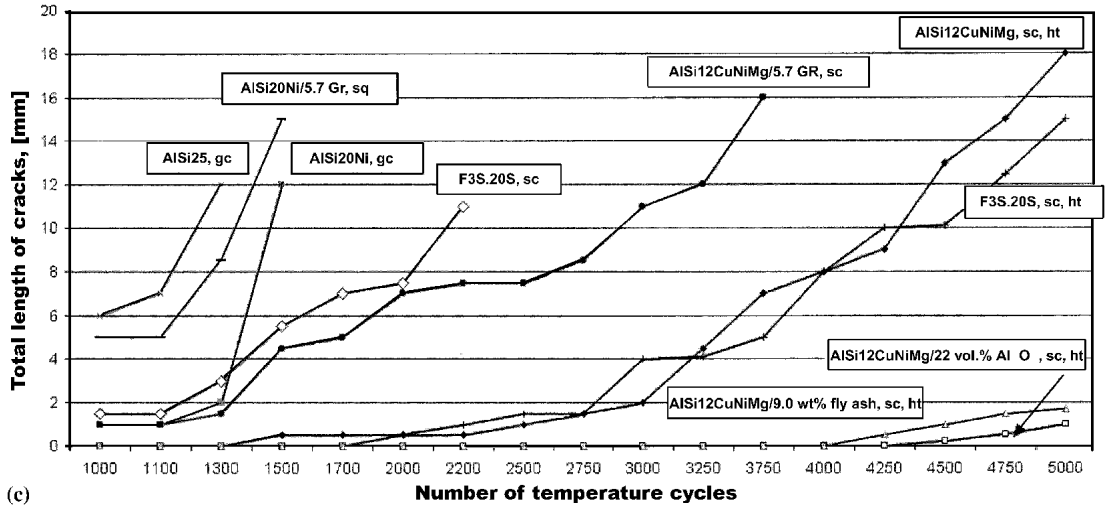

Fig. 2 **(a)** Samples used for thermal shock resistance tests, **(b)** measured temperature cycle during thermal shock tests, and **(c)** thermal shock resistance of the materials investigated in the present work: gc, gravity cast; sc, stir-cast; sq, squeeze cast; and ht, heat treated

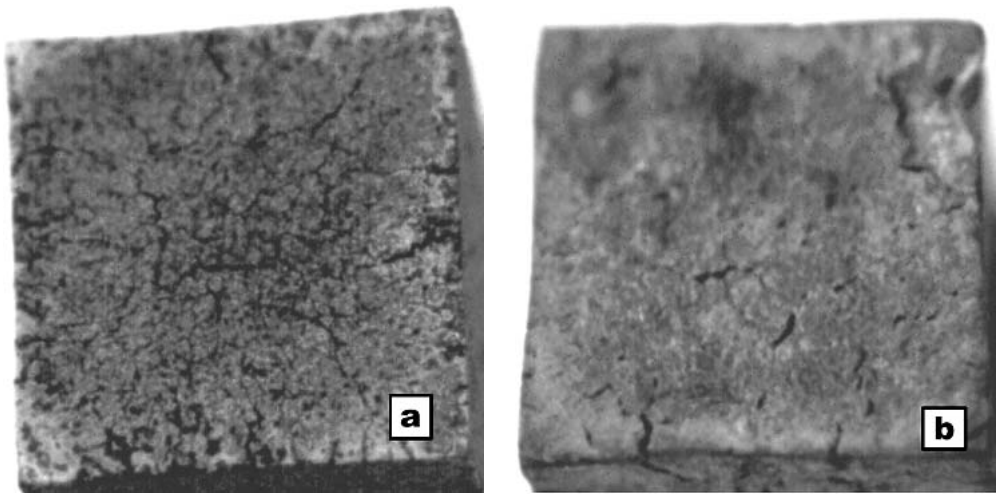

Fig. 3 Test specimen bottom faces in **(a)** AlSi25 gravity cast (1300 cycles), and **(b)** AlSi20 (AK20) gravity cast (1500 cycles) materials

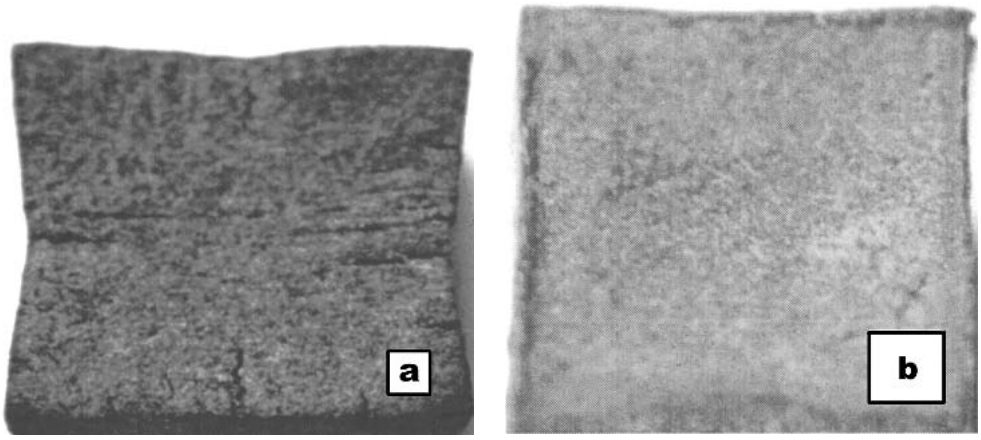

Fig. 4 Test specimen bottom faces in **(a)** AlSi12CuNiMg (AK12) squeeze-cast and heat-treated (T6) alloy (5000 cycles), and **(b)** F3S.20S squeeze cast (as-cast) composite (2200 cycles)

Table 1 Test Materials Used in Thermal Cycling Test

Alloy	Reinforcement (a)
AlSi25	None
AlSi20Ni (AK 20)	None
AlSi12CuNiMg (AK 12)	None
AlSi20Ni	5.7 wt.% graphite (150-200 μm)
A359 (F3S.20S DURALCAN composite)	22 vol.% Sic (~20 μm diameter)
AlSi12CuNiMg	5.7 wt.% graphite
AlSi12CuNiMg	9.0 wt.% precipitator fly ash (b) (50-75 μm)
AlSi12CuNiMg	22 vol.% short Al_2O_3 fiber (c)

(a) The vol.% and wt.% data are taken from either the literature or estimated from quantitative structural analysis. Conversions from wt.% and vol.% or vice-versa are only approximate due to the difficulties in estimating the real density of the reinforcement.
(b) From Dayton Power & Light.
(c) Morgan, United Kingdom, preforms.

ments (Fig. 7b), which include crack propagation: (V) through particle (or fiber), (VI) along the particle (fiber)-matrix boundary, and (VII) across the fiber.

In composites, thermal stresses could be introduced due to temperature gradients and mismatch of coefficients of thermal expansion (CTE) between the reinforcement and the matrix. These stresses could be large, on the order of a few hundred MPa. Additionally, in particulate- and short fiber-reinforced metals, the stress distribution is three-dimensional, and the deformation at high temperatures is likely inhomogeneous (fiber-elastic, matrix-plastic). The matrix could deform plastically near the fiber and elastically away from it, yielding even more complex stress distributions. Due to the CTE mismatch ($\Delta\alpha$), damage is likely to be more severe in the composite than in the unreinforced matrix. The CTE of Al_2O_3 (α-phase), SiC whiskers (β-phase), and Al are approximately 7.7 $\mu m/m \cdot K$, 2.5 $\mu m/m \cdot K$, and 23.5 $\mu m/m \cdot K$, respectively. For $\Delta T = 350$ °C, the thermal strains ($\Delta\alpha\Delta T$) due to CTE mismatch will be approximately 0.00553 for Al_2O_3/Al and 0.00753 for SiC/Al, respectively, and the thermal stresses will be approximately 387 MPa for Al_2O_3/Al, and approximately 527 MPa for SiC/Al, respectively (ignoring the temperature corrections for modulus and CTE). As the yield strength of typical Al alloys is in the range 205-505 MPa, the matrix yield stress might be

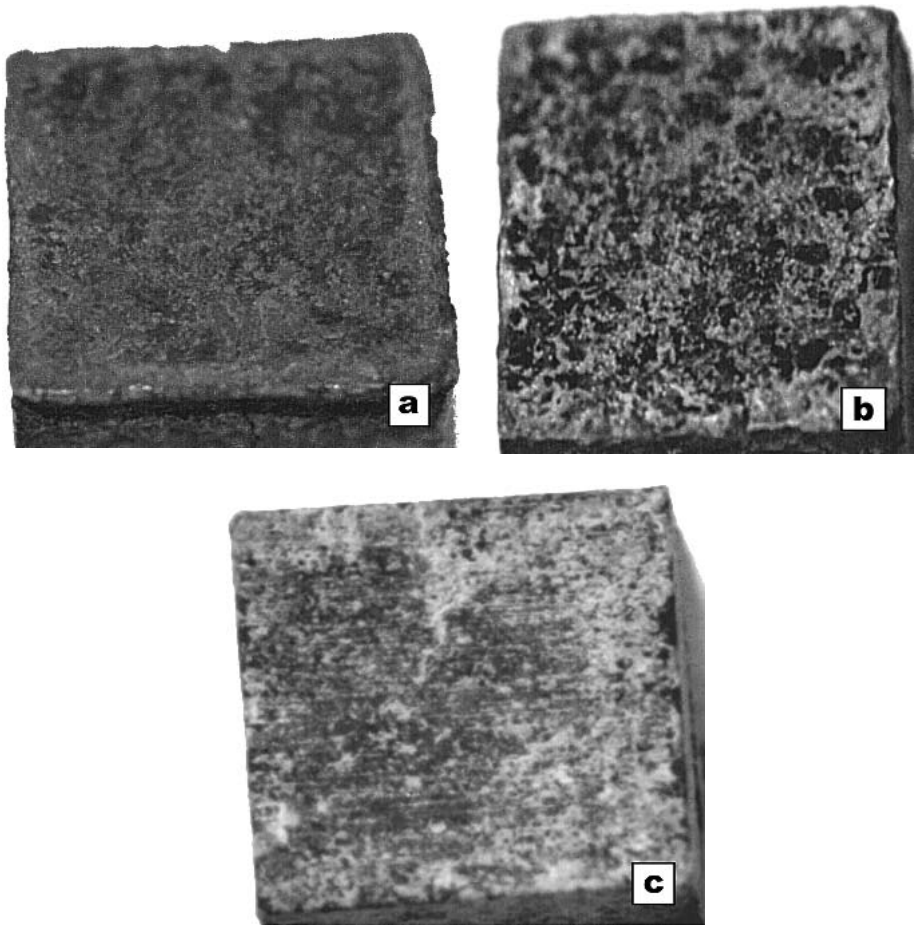

Fig. 5 Bottom faces of test specimens in squeeze cast and heat treated (T6) composites after 5000 thermal cycles: **(a)** F3S.20S, **(b)** AlSi12CuNiMg/9.0% fly ash, and **(c)** AlSi12CuNiMg/22 vol.% Al_2O_3

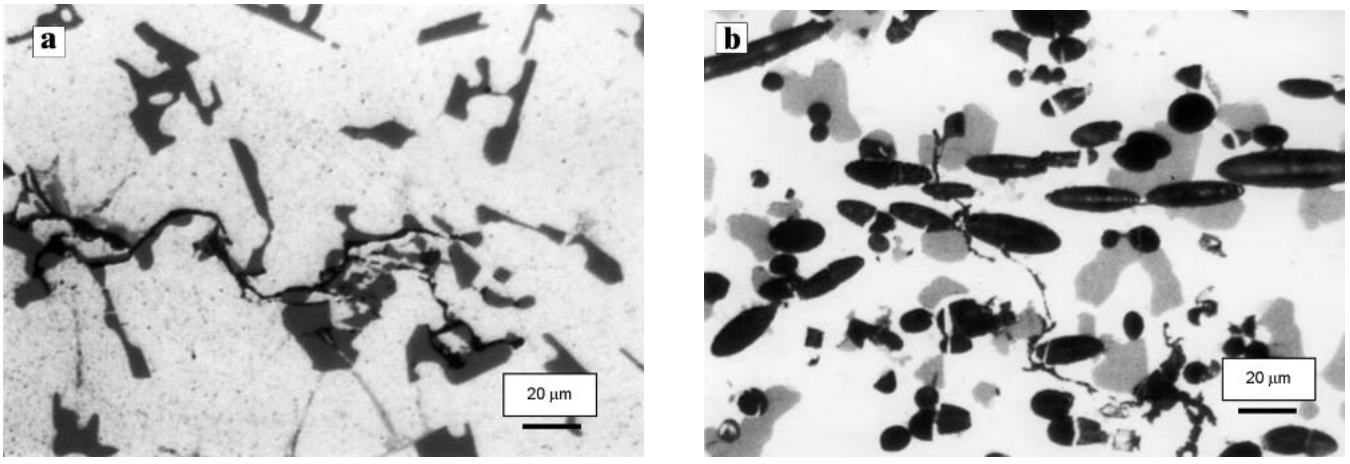

Fig. 6 Microstructures of squeeze-cast and T6 heat-treated **(a)** AlSi12CuNiMg alloy, and **(b)** AlSi12CuNiMg/22 vol.% Al_2O_3 composite after thermal shock resistance tests

reached due to the above temperature excursions. While some stress could be relieved by plastic flow, creep, or interfacial diffusion, residual stresses could be high enough to cause damage in the form of microvoids and interfacial cracks. In spite of a potentially high residual stress, however, the reinforcements (fly ash and alumina short fibers) arrested crack growth, yielding smaller total crack lengths and better thermal shock resistance.

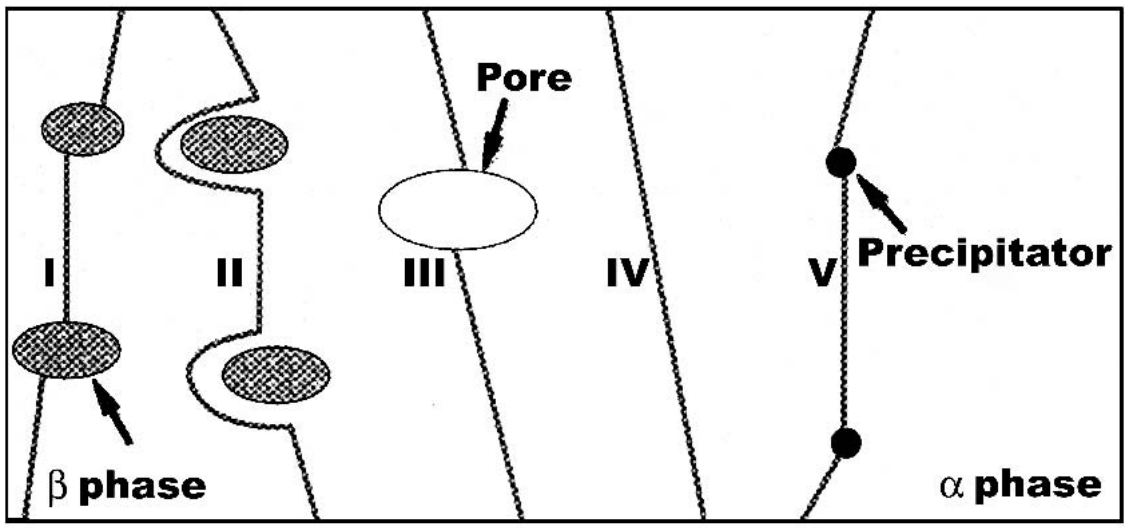

(a)

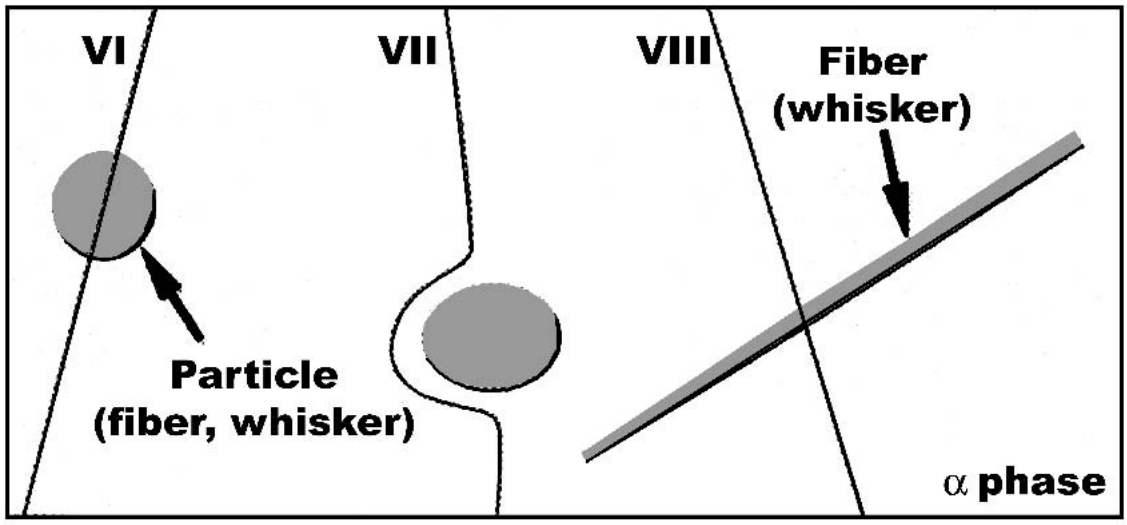

(b)

Fig. 7 Conceptual model for microcrack propagation in **(a)** a monolithic alloy, and **(b)** discontinuously reinforced composite

The thermal shock resistance is characterized in terms of the temperature difference, ΔT, between heating and cooling cycles, which leads to crack formation. This temperature range, ΔT, is $\Delta T = \sigma(1 - \nu)/E\alpha$, where σ is the fracture strength, ν is Poisson's ratio, E is the elastic modulus, and α is the CTE. This equation was used to estimate the fracture strength of squeeze cast and heat-treated (T6) A359/SiC, AK12/fly ash, and AK12/Saffil (alumina) composites. The material property data of Table 2 were used. As a first approximation, either measured or estimated values of E, α, ν, and σ for composites can be used in the above equation. The values of ν and E were estimated from a rule of mixture (ROM), i.e., $\nu_c = \nu_r \cdot \phi + \nu_m.(1-\phi)$, and $E_c = E_r \cdot \phi + E_m.(1-\phi)$, where ϕ is the ceramic volume fraction and the subscripts c, m, and r denote composite, matrix, and reinforcement, respectively.[3] The thermal expansion, α_c, is obtained from Turner's equation,[17]

$$\alpha_c = \frac{\alpha_m(1-\phi).K_m + \alpha_r\phi.K_r}{(1-\phi).K_m + \phi.K_r} \quad \text{(Eq 1)}$$

where K_r and K_m are the bulk moduli of the reinforcement and the matrix, respectively.

Whereas material property data for SiC and Saffil are readily available, the data for fly ash are scarce; as a result,

[3]Note that ROM is strictly valid for a reinforcement that is thermodynamically stable in the metal which is not the case with fly ash in AI. Experimental studies[13] have shown that fly ash reacts with AI, being continuously converted to nanoparticles of alumina via the reaction: $6MeO + 4AI = 2AI_2O_3 + 6Me$, where Me stands for the metal components of oxides that constitute the fly ash. The alumina nanoparticles contribute to the strengthening of the metal matrix and increase the thermal shock resistance of the AI-fly ash composite. The present approach, therefore, purports to be a highly simplified treatment of these complex chemical-mechanical interfacial process.

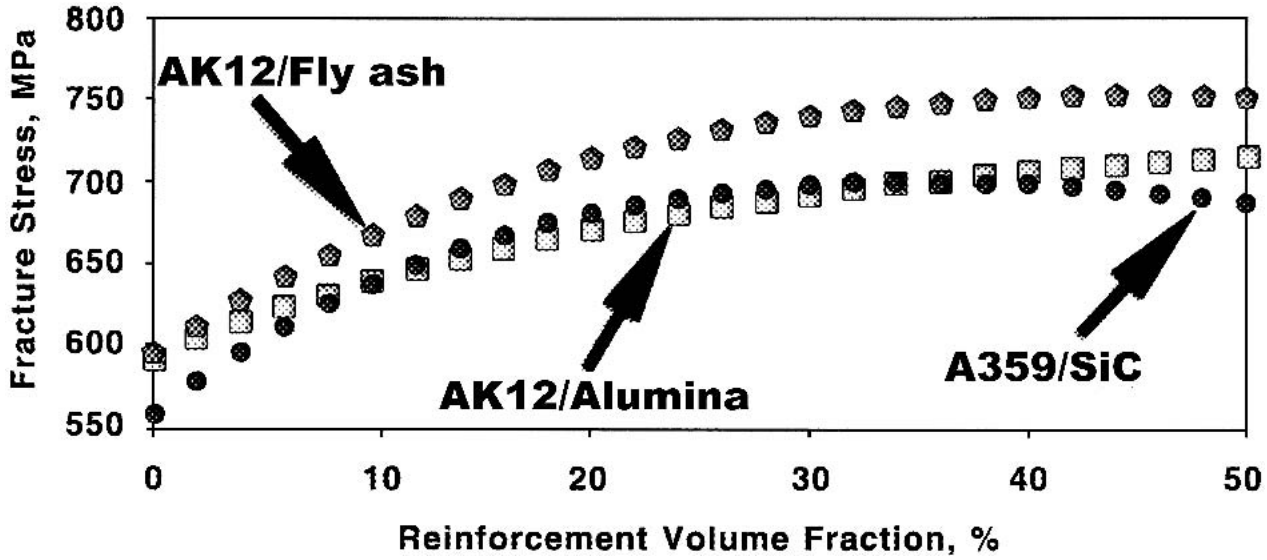

Fig. 8 Calculated fracture stress, σ, of AK12/fly ash, AK12/alumina, and A359/SiC particulate composites

Table 2 Property Data Used in Calculating the Thermal Shock of Composites

	Material (a)				
Property	**A359**	**AK12**	**SiC**	**Saffil**	**Fly ash**
Young's modulus *E*, GPa	75[12]	80[13]	400[14]	285[16]	304 (b)
Poisson's ratio, ν	0.33[12]	0.33[12]	0.17[15]	0.25[14]	0.20 (b)
CTE, μ/m·K	18.4[13]	18.4[13]	4.3[15]	~5.5	5.79 (b)
Bulk modulus (c) *K*, GPa	73.5	78.4	202.1	190	170

(a) ΔT = 270 °C.
(b) Calculated values.
(c) Calculated from the Young's Modulus from: $K = E/3(1-2\nu)$.

properties of fly ash were estimated as described below. First, a Poisson's ratio $\nu_{\text{fly ash}} \approx 0.20$, close to the values for Al_2O_3 and SiO_2 (Table 2), was used. With this and the ROM, the Poisson's ratio of AK12/10.36 vol.% fly ash composite is $\nu_{(10.36)} = 0.317$. Note that the data of Fig. 8 suggest that the fracture strength, σ, of 10.36 vol.% ash composite ≈ σ of 22 vol.% Saffill composite. The calculated fracture strength of AK12/20 vol.% Saffil composite is 705 MPa, which, therefore, will be roughly the fracture strength of AK12/10.36 vol.% fly ash composite.

For AK12/6.71 vol.% (or 5.8 wt.%) precipitator fly ash composite, the following additional data from Ref. 13 were used: $\alpha_{c\ (6.71\%\ ash)} = 16.7$ μm/m. *K* (squeeze cast + T6), $\alpha_{AK12} = 18.4$ μm/m. *K*, $E_{AK12} = 80$ GPa, and $E_{c\ (6.71\%\ ash)} = 95$ GPa. The bulk modulus, *K*, of precipitator fly ash, obtained from $K = E/3(1-2\nu)$, is $0.56E_{\text{fly ash}}$. The application of ROM for modulus to AK12/6.71% ash composite yields *E* of fly ash, $E_{\text{fly ash}}$, as 303.6 GPa. The bulk modulus of fly ash obtained from this value is $K_{\text{fly ash}} = 170$ GPa. To find the thermal expansion of fly ash α_{ash}, Turner's equation (Eq 3) is applied to AK12/6.71% ash composite whose $\alpha_{c\ (6.71\%\text{ash})}$ is given above. This yields α_{ash} as 5.793 μm/m · K. With all the properties of fly ash now known, the thermal shock resistance (i.e., fracture strength, σ) was calculated as a function of the fly ash content in a manner similar to the A359/SiC and AK12/Saffil composites.

Figure 8 represents the calculated fracture strength of the three composites as a function of the reinforcement volume fraction. The results qualitatively agree with the experimental behavior (Fig. 2c). The AK12/Saffil composite has somewhat better thermal shock resistance than the A359/SiC composite (below about 10 vol.% and above about 40 vol.% reinforcement content). The thermal shock resistance of the SiC composite exhibits a minimum within the range of volume fraction investigated. Additionally, the AK12/flyash composite has better crack resistance than A359/SiC composite at all volume fractions, and its fracture strength at 10.36 vol.% ash is similar to the fracture strength of AK12/22 vol.% Saffil composite, as was actually observed in the experiments.

The above calculations of thermal shock resistance are essentially approximate in that they do not consider the heating rate effects and differences in the thermal conductivity of test materials. The failure of brittle materials due to thermal shock is controlled by the elastic stress distribution, by the breaking stress, the heating (and cooling) rates, and the thermal expansion and thermal conductivity. Two parameters that depend upon the heat transfer rates between the body and the environment describe the thermal shock resistance of brittle materials. For high heat transfer rates, the thermal shock resistance (or the maximum tolerable temperature) is $\Delta T_c = \sigma_c(1-\nu)/E\alpha$. On the other hand, for low and moderate heat transfer rates, the thermal shock resistance is given from the second parameter, i.e., $\Delta T_c^* = \sigma_c\ (1-\nu)K/E\alpha$, where σ_c is the breaking stress, ν is the Poisson's ratio, α is the coefficient of thermal expansion (CTE), *E* is the elastic modulus, and *K* is the thermal conductivity.

The effect of heat transfer rates can be estimated from the nondimensional Biot number: $\text{Bi} = r \cdot h/K$, where *r* is a length

scale (usually half thickness or the radius), and h is the interface heat transfer coefficient (heat transferred per unit area per unit temperature difference between the body and the surroundings). If either r or h is very large or if K is very low, Biot number is high, which corresponds to very high heat transfer rates. For very large values of the Biot number, the resistance to thermal shock is essentially independent of h and K, and is estimated from: $\Delta T_c = \sigma_c(1 - \nu)/E\alpha$. The value of h varies over a very wide range, and depends upon the manner in which a body is cooled or heated. On the other hand, low values of Bi correspond to low and moderate heat transfer rates, and the thermal shock resistance is given from: $\Delta T_c^* = \sigma_c(1 - \nu)K/E\alpha$.

Thermal conductivity and thermal expansion are, therefore, important factors affecting the thermal shock resistance, particularly of brittle materials. The thermal conductivity should be high and thermal expansion low for maximum thermal shock resistance. Metals generally have high thermal shock resistance due to their high thermal conductivity and ductility. A low thermal expansion is desirable because it involves low thermal strain and stress. Composites usually possess lower CTE than the matrix alloy: for example, CTE of A359 is 18.4 $\mu m \cdot m^{-1}K^{-1}$ is about 10% greater than the CTE of A360/20%SiC composite (CTE, 16.6 $\mu m \cdot m^{-1}K^{-1}$). On the other hand, compared with metals, different types of composites exhibit substantial difference in the thermal conductivity. For example, the thermal conductivity of the Duralcan composite F3S.20S (A356/20% SiC) is 185 $W \cdot mK^{-1}$, which is about 23% larger than the matrix alloy conductivity (150 $W \cdot mK^{-1}$). Thus, both the lower CTE and higher K of the composite are beneficial to the thermal shock resistance.

The above calculations essentially apply to static or thermal equilibrium situations. They do not accurately represent the dynamic or transient phenomena during thermal cycling.[18] Because the thermal conductivity of the matrix and the reinforcement are widely different, during heating (or cooling) the temperature of the ceramic phase lags behind the matrix, causing different thermal profiles in the two phases. These differences will, in turn, lead to different thermal strains in the two phases, causing additional stresses. In the present simplified treatment, these differences were neglected. In view of this, the calculation of thermal shock resistance offers only a qualitative comparison between different materials, and caution must be exercised in using the calculated values as true or absolute properties.

4. Conclusions

The thermal fatigue resistance of several Al casting alloys and discontinuously reinforced cast Al-matrix composites containing graphite, silicon carbide, fly ash, and alumina was characterized by measuring the total length of microcracks as a function of number of thermal cycles of 270 K amplitude on a specified region of the test specimens. In all specimens, the total crack length increased with increasing number of thermal cycles. Squeezecast Al-alumina and Al-fly ash composites exhibited the best thermal fatigue resistance. Theoretical estimates of the thermal shock resistance of composites, characterized in terms of the fracture strength, qualitatively match the experimental behavior.

References

1. Y.M. Cheong and H.L. Marcus: "In-Situ Thermal Cycling in SEM of a Graphite-Aluminum Composite," *Scripta Mater.*, 1987, *21,* pp. 1529-34.
2. T. Kyono, E. Kurodo, A. Kitamura, T. Mori, and M. Taya: "Effects of Thermal Cycling on Properties of Carbon Fiber/Aluminum Composites," *J. Eng. Mater. Technol (ASME),* 1988, *110,* pp. 89-95.
3. S. Yoda, N. Kurihara, K. Wakashima, and S. Umekawa: "Thermal Cycling Induced Deformation of Fibrous Composites With Particular Reference to the Tungsten/Copper System," *Metall. Trans.,* 1978, *9A,* pp. 1229-36.
4. H.H. Grimes, R.A. Lad, and J.E. Masial: "Thermal Degradation of Tensile Strength of Unidirectional Boron/Al Composites," *Metall. Trans*., 1977, *8A,* pp. 1999-2005.
5. A.K. Misra: "Effect of Thermal Cycling on Interface Bonding Requirements in Alumina Fiber-Reinforced Superalloy Composites," *Scripta Mater.,* 1993, *28,* pp. 1189-94.
6. W.H. Kim, M.J. Koczak, and A. Lawley: "Effects of Isothermal and Cyclic Exposure on Interface Structure and Mechanical Properties of FP-Alumina/Al Composite" in *New Developments and Applications in Composites*, D. Kuhlmann-Wilsdorf and W.C. Harrigan, Jr., ed., TMS of AIME, Warrendale, PA, 1979, pp. 40-53.
7. W.G. Patterson and M. Taya: "Thermal Cycling Damage of SiC Whisker/2124 Al Aluminum" in *Proceedings of International Conference on Composite Materials (ICCM-V)*, W.C. Harrigan, Jr., et al., ed., TMS of AIME, Warrendale, PA, 1985, pp. 53-66.
8. M. Nakanishi, Y. Nishida, H. Matsubara, M. Yamada, and Y. Tozawa: "Effect of Thermal Cycling on the Properties of SiC Whisker Reinforced-Aluminum Alloys," *J. Mater. Sci. Lett*., 1990, *9,* pp. 470-72.
9. F. Rezai-Aria, T. Liechti, and G. Gagnon: "Thermal Cycling Behavior of a Pure Al-15% Saffil MMC," *Scripta Mater.*, 1993, *28,* pp. 587-92.
10. W. Hennig, C. Meltzer, and S. Mielke: "Keramische Gradienenwerkstoffe für Komponenten in Verbrennungsmotoren," *Metall.*, 1992, *Hf.5, J.46,* pp. 436-39 (in German).
11. J. Sobczak: "Metal-Matrix Composites Fabricated by the Squeeze Casting Process," *Trans. Foundry Res. Inst. (Special Issue)*, Krakow, 1993, *415,* pp. 1-99.
12. Anon: "Properties and Selection: Nonferrous Alloys & Special-Purpose Materials," *Metals Handbook*, Vol. 2, 10th ed., ASM International, Materials Park, OH, 1990, pp. 152-77.
13. N. Sobczak, J. Sobczak, and P.K. Rohatgi: "Using Fly Ash Waste Material for the Synthesis of Light-Weight, Low-Cost Al-Matrix Composites" in *Proceedings of ECOMAP-98*, High-Temperature Society of Japan, Kyoto, Japan, 1998, pp. 195-204.
14. A.L. Geiger and M. Jackson: "Low Expansion MMC's Boost Avionics," *Adv. Mater. Proc.*, 1989, *7,* pp. 23-30.
15. D.J. Lloyd: "Particulate Reinforced Al and Mg Composites," *Int. Mater. Rev.*, 1994, *39*(1), pp. 1-27.
16. M. Taya and R.J. Arsenault: *Metal Matrix Composite–Thermomechanical Behavior*, Pergamon Press, New York, NY, 1989, p. 245.
17. R.U. Vaidya and K.K. Chawla: "Thermal Expansion of Metal-Matrix Composites," *Comp. Sci. Technol.*, 1994, *50,* pp. 13-22.
18. C.H. Lee: "Dynamic Mismatch Between Bonded Dissimilar Materials," *JOM*, Jun 1993, pp. 43-46.